Supporting information

Tunable mixed oxides based on CeO_2 for the selective aerobic oxidation of 5-(hydroxymethyl)furfural to FDCA in water

Maria Ventura,[a] Francesco Nocito,[b] Elvira de Giglio,[b] Stefania Cometa,[c] Angela Altomare,[d] Angela Dibenedetto,[a,b]*

[a]CIRCC, Via Celso Ulpiani, 27, 70126 Bari, Italy; [b]Department of Chemistry, University of Bari, Campus Universitario, 70126 Bari, Italy; [c]Jaber Innovation srl, Via Calcutta 8, Rome, Italy; [d]Crystallography Institute-CNR, Via Giovanni Amendola, 122/O, 70126 Bari, Italy.

List of contents

Experimental part

Materials and methods

Cerium ammonium nitrate ≥98% (by titration); manganese (IV) oxide 99.99% trace metal basis; 2,5-furandicarboxaldehyde ≥97%; 5-formyl-2-furoic acid 99%; 5-hydroxymethyl-2-furancarboxylic acid 99%, 2,5-furandicarboxylic acid 99%, were ACS grade reagents purchased from Sigma Aldrich. 5-(hydroxymethyl)furfural was prepared as we reported in ref. 5.

5-HMF and derivatives were analyzed by using a Jasco HPLC equipped with a RI detector and a Phenomenex Rezex RHM Monosaccharide H^+(8%) 300x7.8mm at 343 K. A 0.005 N solution of sulphuric acid was used as the mobile phase. The flow rate was between 0.5-0.9 mL/min. The concentration of 5-HMF and reaction products were determined using a RI detector. DFF concentration was analysed in ethyl acetate solution, using a Thermo Scientific GC with initial temperature of 323 K for 2 min. The rate of the first ramp was 7 ºC/min until 393 K for 8 min. The second ramp rate was 15 ºC/min until 403 K for 10 min.

Energy Dispersive X-ray diffraction (EDX) patterns were recorded at room temperature on a Shimadzu EDX-720/800 HS, using a 5 to 50 kV Rh target x-ray generator and a Si (Li) detecting system. For noise reduction, the detector was cooled using liquid nitrogen.

Flameless Atomic Absorption Spectroscopy-FLAAS was carried out with a Perkin Elmer apparatus.

X-ray Photoelectron Spectroscopy (XPS) analysis was performed by a scanning microprobe PHI 5000 VersaProbe II (Physical Electronics, Chanhassen, MN), equipped with a monochromatized AlKα X-ray radiation source. High-resolution spectra (FAT mode, pass energy 29.35 eV) were recorded for each sample and data analysis was performed using the MultiPak software package (version 9.6.1.7). The normalization of the peak area and comparison of data from different elements was enabled by correction with empirically derived sensitivity factors according to MultiPak library.

Specific Surface Areas were determined with a Micromeritics Chemisorb 2750 equipment (BET method). The analyses of the acid and basic sites were carried out using NH_3 and CO_2, respectively, as probe-gas with 100 mg of catalyst. The samples

were pre-treated under N_2 flow (30 mL min^{-1}) at 823 K. The Pulse Chemisorb was performed using He as carrier gas (30 mL min^{-1}). The TPD analyses were performed under He flow at 30 mL min^{-1}.

Powder X-ray diffraction (PXRD) patterns were recorded at room temperature on a Bruker D8-DISCOVER [Bruker AXS. Karlsruhe, Germany] powder diffractometer equipped with a Göbel Mirror for Cu Kα radiation ($\lambda_{K\alpha1}$= 1.54056 Å e $\lambda_{K\alpha2}$= 1.54439 Å). The working conditions were 40kV and 50 mA. Data were collected in the 2θ range between 10° and 120°, with a 0.05° step size and a counting time of 1s per step, with 2θ/ω scan type.

Catalysts preparation

(a) Synthesis of $MnO_2 \cdot CeO_2$

Cerium(IV) ammonium nitrate (1 mmol; 0.54 g), and manganese (IV) oxide (1 mmol; 0.08 g), were mixed in a High Energy Milling-HEM apparatus and pulverized at 790 rpm during 1 h with pauses of 1 min every 15 min and inversion of the rotation sense. The black mixture was calcined for 3 h at 723-923 K. The solid was transferred into a flask and stored under N_2 atmosphere to prevent uncontrolled surface deterioration prior to catalysis. The data for the elemental analysis carried out by EDX are shown in Table S1.

(b) Synthesis of $CuO \cdot MnO_2 \cdot CeO_2$

An equivalent amount of cerium (IV) ammonium nitrate (1 mmol; 0.54 g), manganese (IV) oxide (1 mmol; 0.08 g), and copper nitrate (1 mmol), were mixed in a High Energy Milling-HEM apparatus following the procedure described in (a). The solids were transferred in a flask and stored under N_2 atmosphere to prevent uncontrolled surface deterioration prior to catalysis. The data for the elemental analysis carried out by EDX are shown in Table S1.

Catalytic tests and product analysis

(c) The kinetics of conversion of 5-HMF at a fixed temperature, was studied in a 50 mL stainless-steel reactor equipped with a withdrawal valve and an electrical heating jacket. 1 mmol of 5-HMF (0.126 g) was dissolved in 7 mL of distilled water in a glass reactor, in which 0.05 g of the catalyst under study and a magnetic stirrer were placed. The glass-reactor was then transferred into the autoclave that was closed and purged

three times with O_2. It was charged with the appropriate pressure of oxygen and heated to the reaction temperature as specified in Results and Discussion. At fixed intervals of time, stirring was stopped, a sample of the solution was withdrawn and analysed by HPLC following the disappearance of 5-HMF. When the concentration of the latter dropped to a constant value (or even zero), the reaction was stopped. The solution and the solid were extracted three times with 7 mL of ethyl acetate (EtOAc) and the EtOAc phases were collected. This procedure was necessary because DFF is only slightly soluble in water and can precipitate in the reaction medium. The collected EtOAc phase was washed with water to remove 5-HMF dissolved into it, dried with Na_2SO_4, filtered and analysed by GC. Evaporation in vacuum of EtOAc gave the pure DFF (98% yield).

(d) In order to test whether oxygen was originated from the metal oxides or gas phase, 5_HMF was treated with the catalyst in absence of oxygen in the same conditions described in (c) and the products characterised as reported above.

Analytical methods

5-HMF and derivatives were analyzed by using a Jasco HPLC equipped with a RI detector and a Phenomenex Rezex RHM Monosaccharide H+(8%) 300x7.8mm at 343 K. A 0.005 N solution of sulphuric acid was used as the mobile phase. The flow rate was between 0.5-0.9 mL/min. The concentration of 5-HMF and reaction products were determined using a RI detector. DFF concentration was analysed in ethyl acetate solution, using a Thermo Scientific GC with initial temperature of 323 K for 2 min. The rate of the first ramp was 7 ºC/min until 393 K for 8 min. The second ramp rate was 15 ºC/min until 403 K for 10 min.

Surface characterization of the catalysts was carried out by using the Pulse ChemiSorb 2750 Micromeritics instrument. Analyses of the acidic/basic sites were carried out using NH_3 or CO_2, respectively, as probe-gas using 100 mg of catalyst. The samples were pre-treated under N_2 (30 mL min^{-1}) flow at 673 K. The Pulse Chemisorb was performed with NH_3 or CO_2 gas using He as carrier gas (30 mL min^{-1}). Specific Surface Area was determined using Brunauer Emmett Teller (BET) method and N_2/He as carrier gas at 273 K followed by heating up to 923 K. Temperature Programmed Desorption (TPD) were performed under He flow at 30 mL min^{-1}. H_2-TPR analyses were carried out by using a mixture of H_2/Ar as carrier gas (30 mL min^{-1}) at 300 K, the sample was heated up to 1273.15 K.

The X-ray powder diffraction patterns were collected at room temperature using an automated Rigaku RINT2500 diffractometer (50 KV, 200 mA) equipped with the silicon strip Rigaku D/teX Ultra detector (IC-240 CNR, Bari). An asymmetric Johansson Ge crystal was used to select the monochromatic Cu Kα1 radiation (λ= 1.54056 Å). The measurements were executed in transmission mode, by introducing the samples in special glass capillaries with a 0.3 mm of diameter and mounted on the axis of the diffractometer. In order to reduce the effect of possible preferred orientation, the capillaries were rotated during measurements to improve the randomization of the orientations of the individual crystallites.

Tables and Figures

Table S1. Elemental analyses by EDX for the mixed oxides.

Entry	Solid	Theoretical % of oxide			Experimental % of oxide		
		%Mn	%Ce	%M	%Mn	%Ce	%M
1	$MnO_2{\cdot}CeO_2$	21.20	54.8	-	20.18	54.12	-
2	$CuO{\cdot}MnO_2{\cdot}CeO_2$	16.22	41.38	18.76	16.52	41.25	19.84

Table S2. Surface atomic concentration of Mn/Ce before and after reaction

Entry	Element	Atomic %	Ratio Ce/Mn	
1	O1s	56.6		
2	Ce3d	12.5	1.3	Before reaction
3	Mn2p	9.9		
4	O1s	44.2		
5	Ce3d	8.9	1.7	After reaction
6	Mn2p	5.3		

Table S3. Surface atomic concentration of Cu/Mn/Ce before and after reaction

Entry	Element	Atomic %	Ratio Mn/Ce/Cu	
1	O1s	44.4		
2	Ce3d	4.2	3.2:1.1:1	Before reaction
3	Mn2p	11.8		
4	Cu2p	3.7		
5	O1s	49.7		
6	Ce3d	7.1	3.2:2.8:1	After reaction
7	Mn2p	8.0		
8	Cu2p	2.5		

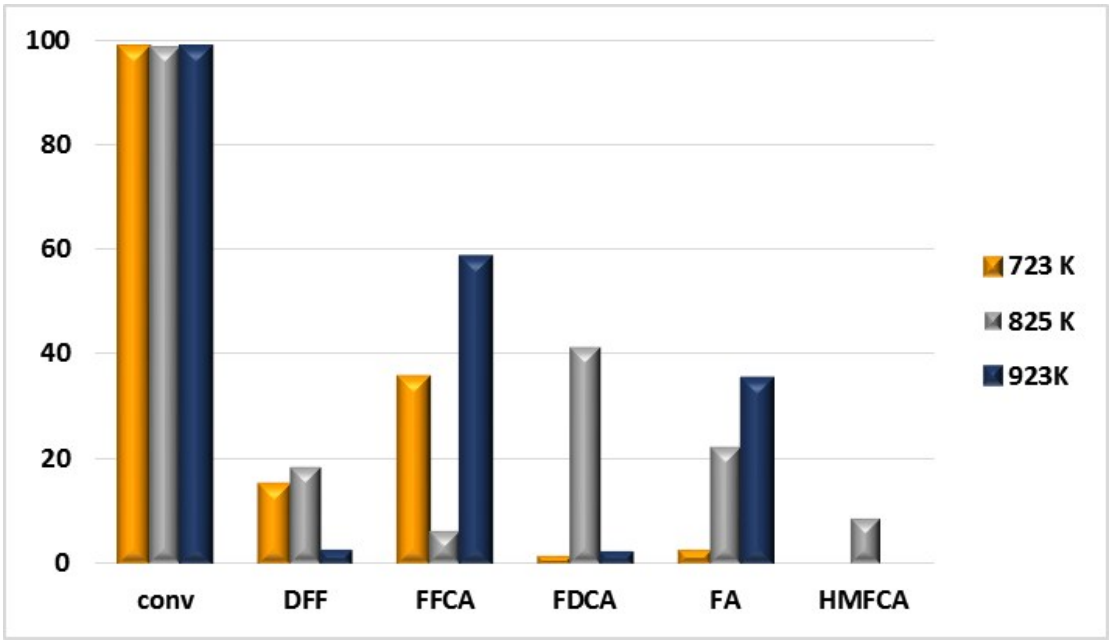

Reaction conditions: 0.05 g of catalyst, P_{O_2}=9MPa, temperature=403K, $[HMF]_i$=0.2M

Figure S1. Oxidation of 5-HMF: Comparison of the activity of $MnO_2{\cdot}CeO_2$ mixed oxide calcined at different temperatures.

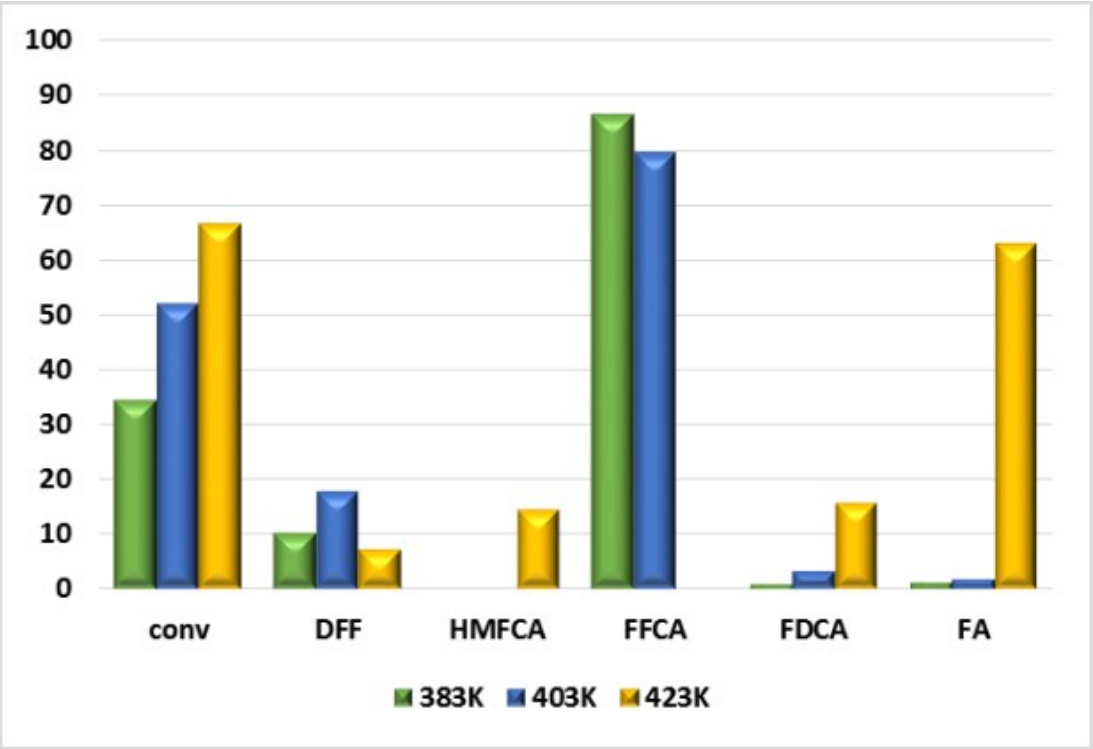

Figure S2. Oxidation of 5-HMF with $(MnO_2 \cdot CeO_2)_{825K}$ mixed oxide at different temperatures at 1h of reaction

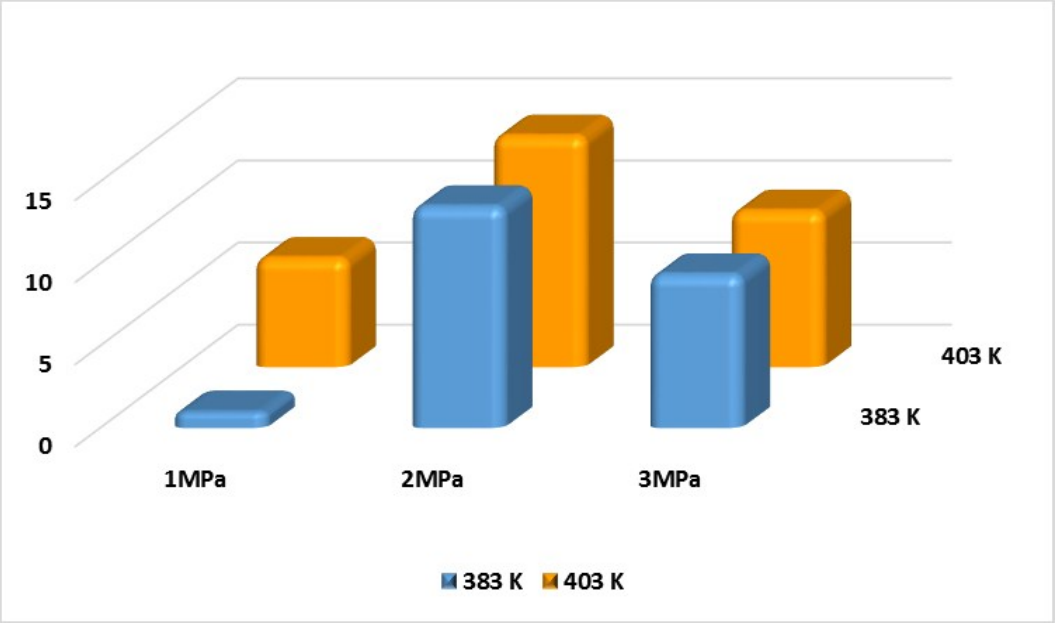

Reaction conditions: 0.05 g of catalyst, $[HMF]_i$=0.2M, time=3h.

Figure S3. Selectivity towards FDCA at different pressures and temperatures. Y-axis gives the % yield of products. X-axis gives the pressure. Two sets of data are compared T 383 and 403 K.

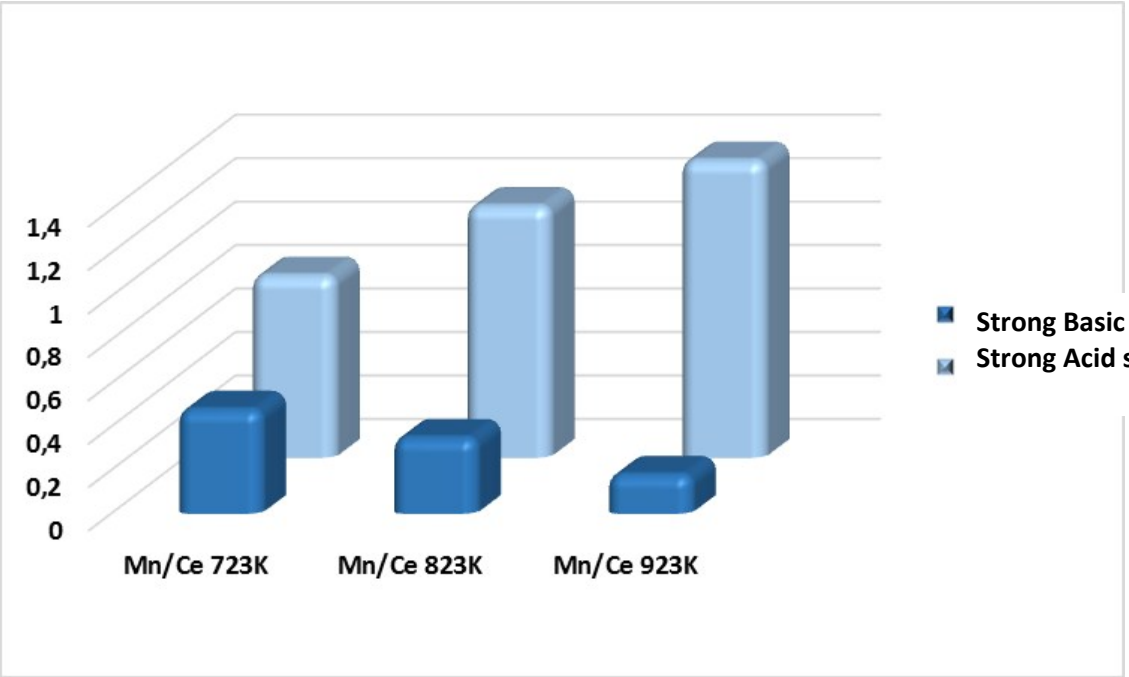

Figure S4. Change of the acidic/basic sites with the change of the calcination temperature. Y-axis gives the ratio n_b/n_a of strong acidic to basic sites calculated through the amount of released NH_3 or CO_2, respectively. Increasing the temperature of calcination causes an increase of n_b/n_a from 3.7 to >11.

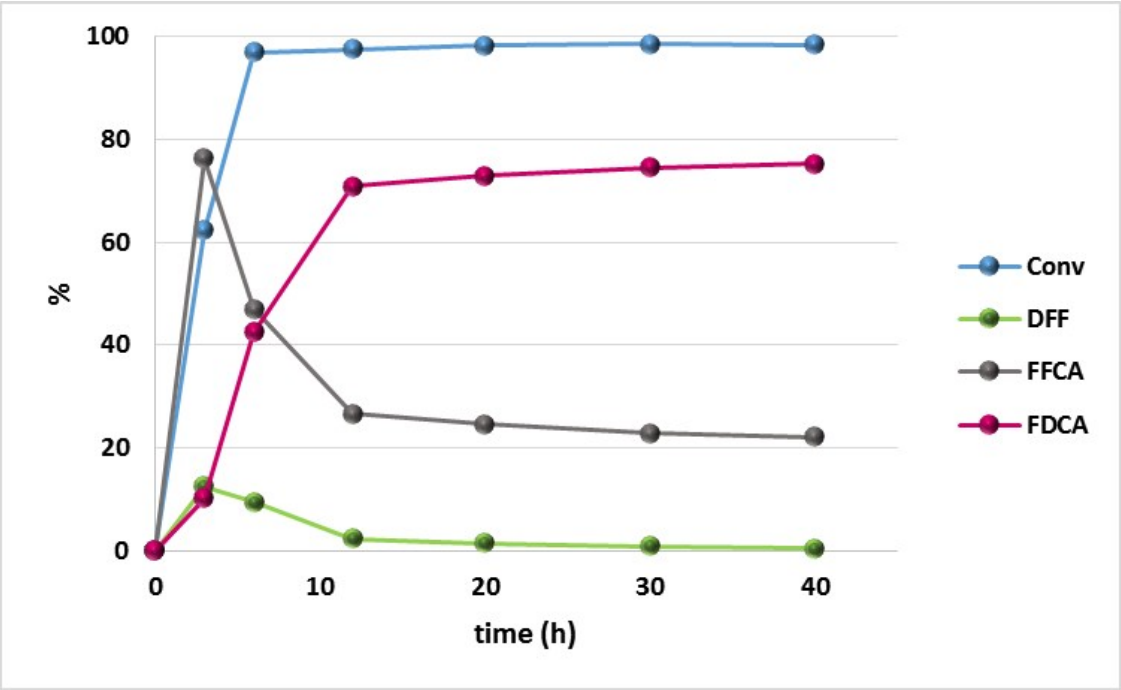

Figure S5. Kinetics of the reaction performed using $CuO{\cdot}MnO_2{\cdot}CeO_2$ mixed oxide as catalyst.

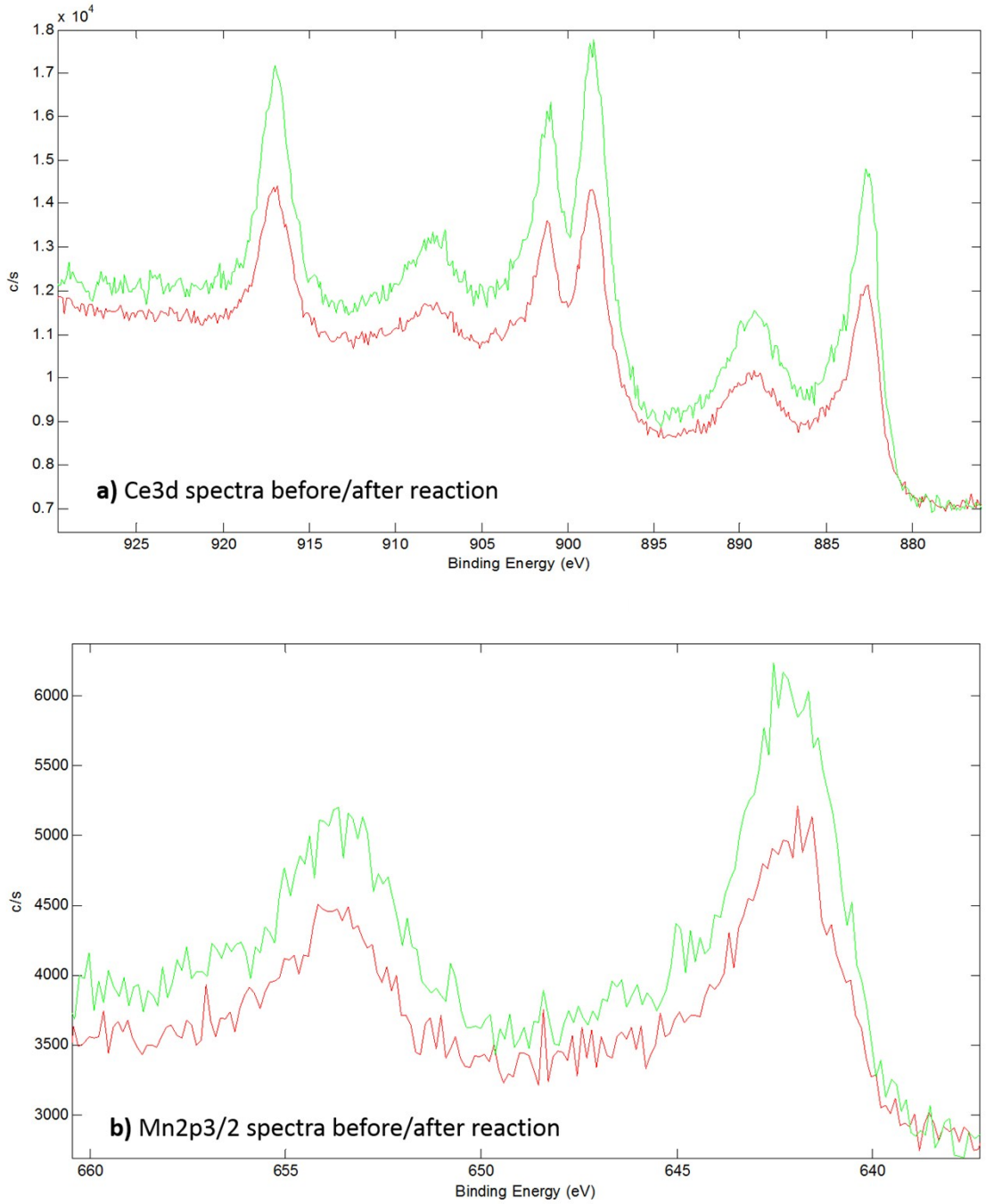

Figure S6. XPS spectra of $MnO_2 \cdot CeO_2$ before (green line) and after (red line) reaction.

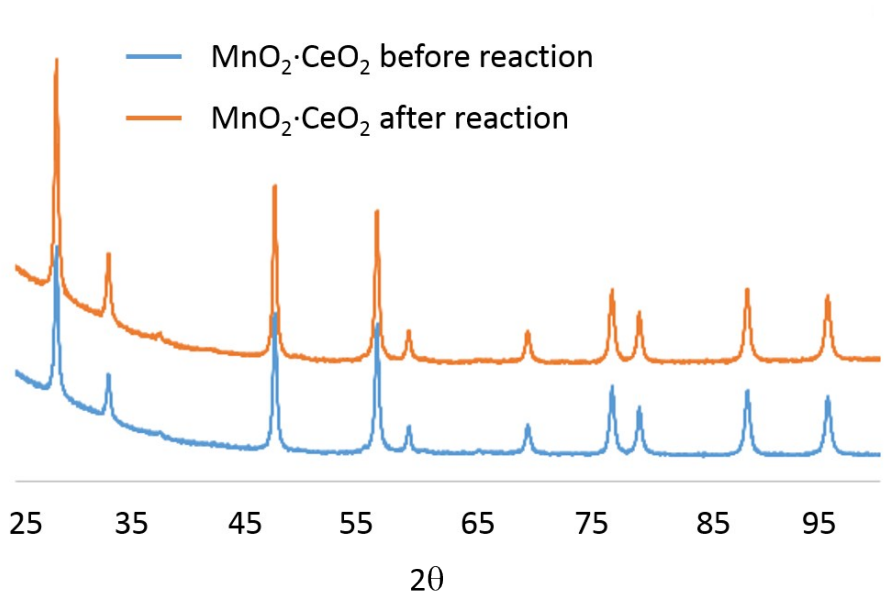

Figure S7. XRD pattern of $MnO_2 \cdot CeO_2$ mixed oxide before and after reaction.

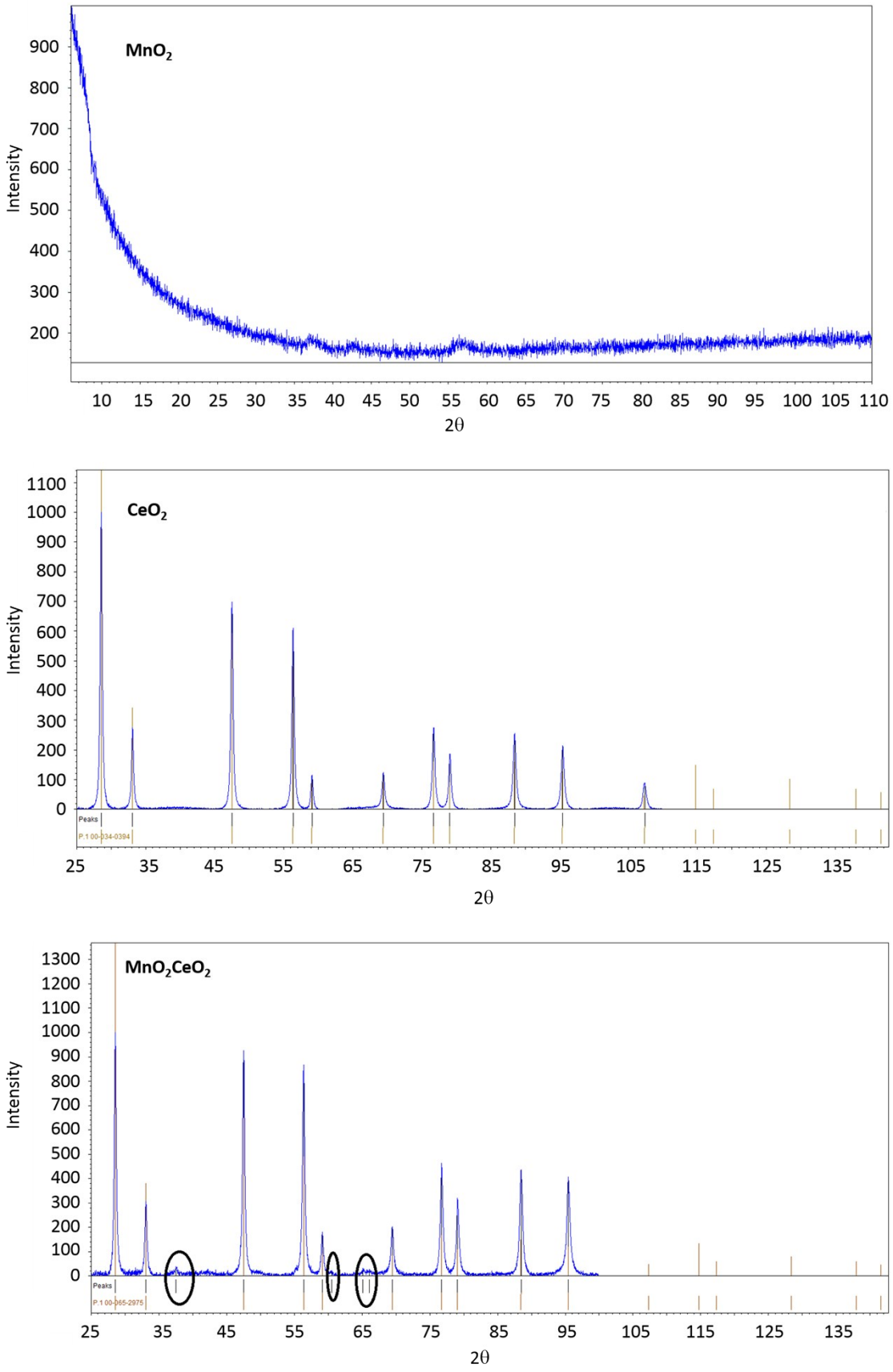

Figure S8. XRD patterns of single (MnO_2, CeO_2) and mixed oxides ($MnO_2 \cdot CeO_2$).

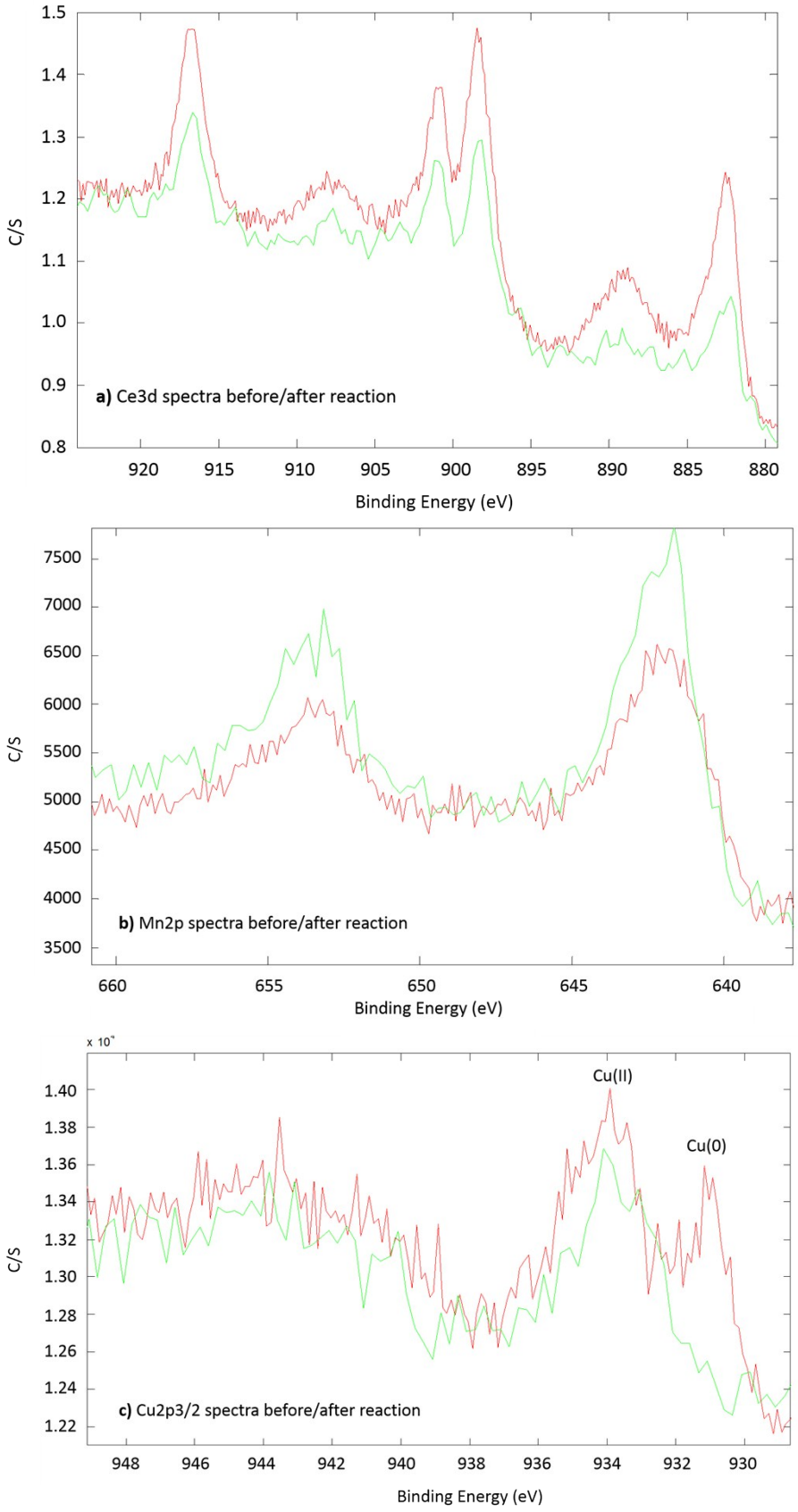

Figure S9. XPS spectra of $CuO{\cdot}MnO_2{\cdot}CeO_2$ before (green line) and after (red line) reaction

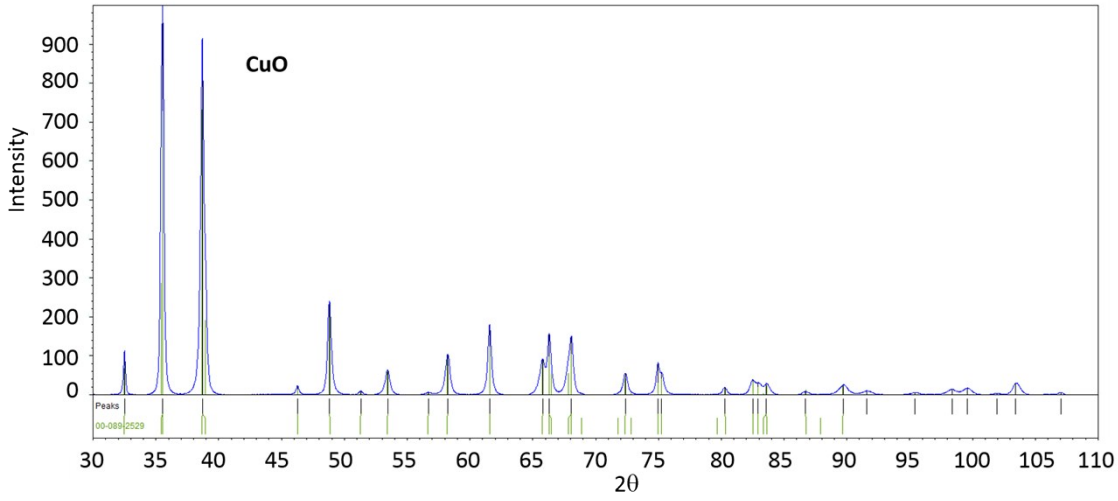

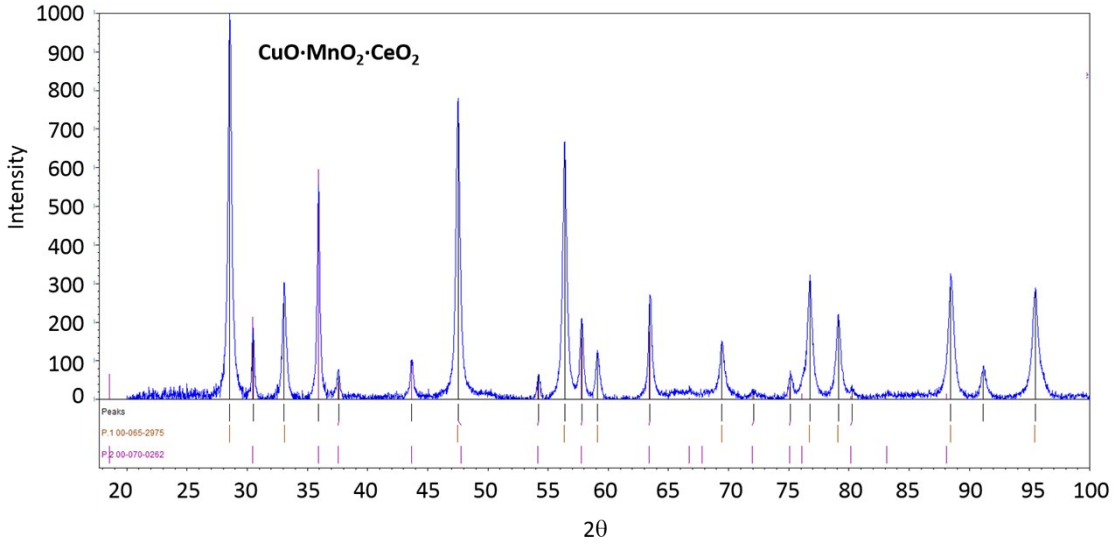

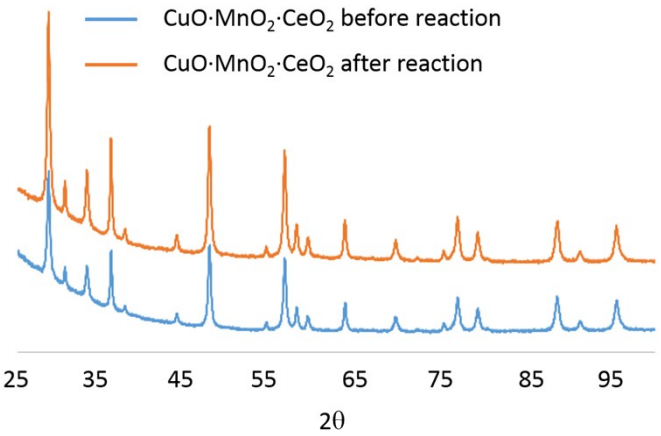

Figure S10. XRD patterns of single (CuO), mixed oxides ($CuO{\cdot}MnO_2{\cdot}CeO_2$) and XRD pattern of the mixed oxide ($CuO{\cdot}MnO_2{\cdot}CeO_2$) before and after reaction.